The FASEB Journal • Research Communication

Genome-wide association mapping of acute lung injury in neonatal inbred mice

Jennifer L. Nichols,*,† Wesley Gladwell,* Kirsten C. Verhein,* Hye-Youn Cho,* Jürgen Wess,§ Oscar Suzuki,‡ Tim Wiltshire,‡ and Steven R. Kleeberger*,[1]

*Laboratory of Respiratory Biology, National Institute of Environmental Health Sciences, U.S. National Institutes of Health, Research Triangle Park, North Carolina, USA; †Curriculum in Toxicology, Center for Environmental Medicine, Asthma, and Lung Biology, and ‡Division of Pharmacotherapy and Experimental Therapeutics, Eshelman School of Pharmacy, University of North Carolina, Chapel Hill, North Carolina, USA; and §Laboratory of Bioorganic Chemistry, National Institute of Diabetes and Digestive and Kidney Diseases, U.S. National Institutes of Health, Bethesda, Maryland, USA

ABSTRACT **Reactive oxygen species (ROS) contribute to the pathogenesis of many acute and chronic pulmonary disorders, including bronchopulmonary dysplasia (BPD), a respiratory condition that affects preterm infants. However, the mechanisms of susceptibility to oxidant stress in neonatal lungs are not completely understood. We evaluated the role of genetic background in response to oxidant stress in the neonatal lung by exposing mice from 36 inbred strains to hyperoxia (95% O_2) for 72 h after birth. Hyperoxia-induced lung injury was evaluated by using bronchoalveolar lavage fluid (BALF) analysis and pathology. Statistically significant interstrain variation was found for BALF inflammatory cells and protein (heritability estimates range: 33.6–55.7%). Genome-wide association mapping using injury phenotypes identified quantitative trait loci (QTLs) on chromosomes 1, 2, 4, 6, and 7. Comparative mapping of the chromosome 6 QTLs identified *Chrm2* (cholinergic receptor, muscarinic 2, cardiac) as a candidate susceptibility gene, and mouse strains with a nonsynonymous coding single-nucleotide polymorphism (SNP) in *Chrm2* that causes an amino acid substitution (P265L) had significantly reduced hyperoxia-induced inflammation compared to strains without the SNP. Further, hyperoxia-induced lung injury was significantly reduced in neonatal mice with targeted deletion of *Chrm2*, relative to wild-type controls. This study has important implications for understanding the mechanisms of oxidative lung injury in neonates.—Nichols, J. L., Gladwell, W., Verhein, K. C., Cho, H.-Y., Wess, J., Suzuki, O., Wiltshire, T., Kleeberger, S. R. Genome-wide association mapping of acute lung injury in neonatal inbred mice. *FASEB J.* 28, 2538–2550 (2014). www.fasebj.org**

Key Words: bronchopulmonary dysplasia · inflammation · quantitative trait locus · cholinergic receptor · muscarinic 2 · cardiac

Bronchopulmonary dysplasia (BPD) is a chronic respiratory disease that is associated with prematurity and an underdeveloped pulmonary system (1, 2). Because the lung does not reach maturation until after birth, babies born prematurely are frequently incapable of adequate ventilation and gas exchange (1, 3). To compensate, respiratory support with supplemental oxygen and/or mechanical ventilation is used until respiration can be maintained independently (4). Despite the success of this strategy, subsets of infants are adversely affected and may develop BPD. Although the mechanisms are poorly understood (5, 6), the combination of developmental immaturity and ventilator support in these infants results in impaired alveolarization and abnormal vascularization, and decreased respiratory function has been reported beyond childhood (7, 8).

Initial efforts to understand differential susceptibility to BPD revealed a strong genetic component (9); clinical studies in twins reported heritability estimates ranging from 53 to 82% (10, 11). Although genetic studies have found associations between disease and genetic variants in pathological processes underlying BPD, including inflammation, antioxidant defense,

Abbreviations: ANOVA, analysis of variance; BAL, bronchoalveolar lavage; BALF, bronchoalveolar lavage fluid; BPD, bronchopulmonary dysplasia; *Cyp2j*, cytochrome P450; family 2, subfamily j; *Chrm2*, cholinergic receptor, muscarinic 2, cardiac; EMMA, efficient mixed-model association; GWA, genome-wide association; H&E, hematoxylin and eosin; HBSS, Hanks' balanced salt solution; *Hsnl*, hyperoxia susceptibility in neonatal lungs; *Mgmt*, *O*-6-methylguanine-DNA methyltransferase; PMN, polymorphonuclear leukocyte; PPAR, peroxisome proliferator-activated receptor; QTL, quantitative trait locus; ROS, reactive oxygen species; SNP, single-nucleotide polymorphism

[1] Correspondence: National Institute of Environmental Health Sciences, 111 T. W. Alexander Dr., Bldg. 101, MD-201, Research Triangle Park, NC 27709, USA. E-mail: kleeber1@niehs.nih.gov

doi: 10.1096/fj.13-247221

This article includes supplemental data. Please visit *http://www.fasebj.org* to obtain this information.

0892-6638/14/0028-2538 © FASEB

lung development, and vascular development (7, 10, 12, 13), these studies are limited by small sample sizes, confounding variables (3), lack of reproducibility, and phenotypic heterogeneity and polygenicity (14, 15). Therefore, appropriate animal models are needed to better understand key events in late lung development during the transition from saccularization to alveolarization and the factors that contribute to BPD (2). Although models are reported in various species (16–18), mice are invaluable for genetic studies. In addition, there is concordance between BPD phenotypes and hyperoxic lung injury in neonatal mice, as hyperoxia augments reactive oxygen species (ROS) formation (19, 20), and neonatal exposure can produce similar impaired alveolarization and reduced lung function in adolescence (21–23).

Currently, genetic determinants of susceptibility to neonatal hyperoxic lung injury are not completely understood. Haplotype association mapping approaches in inbred strains of mice have yielded many important findings that have contributed significantly to our understanding of the genetic basis of susceptibility to several diseases (24). In the current study, our first objective was to establish a genetic neonatal model of hyperoxic lung injury in inbred strains of mice. The second objective was to use the injury phenotypes for genome-wide association (GWA) mapping to identify quantitative trait loci (QTLs) and candidate susceptibility genes that associate with neonatal hyperoxic lung injury.

MATERIALS AND METHODS

Animals and hyperoxia exposure

Male and female mice (4–10 wk) from 36 inbred strains were purchased from the Jackson Laboratory (Bar Harbor, ME, USA). Mice with targeted deletion of *Chrm2* (cholinergic receptor, muscarinic 2, cardiac; 129S4/SvJaeJ X CF-1 F_1-$Chrm2^{-/-}$) and wild-type (129S4/SvJaeJ X CF-1 F_1-$Chrm2^{+/+}$) mice were obtained from the National Institute of Diabetes and Digestive and Kidney Diseases (Bethesda, MD, USA). Development of the $Chrm2^{-/-}$ mice and the effect of the deletion on expression in the lung have been described previously (25, 26). The mice were caged individually at the National Institute of Environmental Health Sciences (NIEHS) facility, maintained in a 12-h light-dark cycle at 72°F with 50% humidity, and provided food and water *ad libitum*. The animals were acclimated to these conditions for a week before mating. The males and females were housed together for 3–5 d; after cohabitation, the males were removed, and 1–3 of the females were housed per cage until pregnancy was confirmed. At 12–24 h after spontaneous birth, pups from multiple litters were pooled and randomly assigned to air or hyperoxia exposure groups. The litters from all strains were cross-fostered with Swiss Webster dams (Charles River, Wilmington, MA, USA) to ensure adequate and consistent maternal care. The litters with foster dams were maintained in room air or a chamber supplied with ≥95% oxygen (UHP grade, minimum purity 99.994%; National Welders, Durham, NC, USA) for 72 h. The chamber was opened for 30 min each morning for health checks, cage cleaning, and cross-fostering. After termination of exposure, the mice were weighed and euthanized by i.p. injection of pentobarbital sodium (104 mg/kg). Animal procedures were approved by the NIEHS Institutional Animal Care and Use Committee.

Bronchoalveolar lavage (BAL)

After the neonates were euthanized, the whole lung of each one was lavaged *in situ* 4 times with 100 μl Hanks' balanced salt solution (HBSS; pH 7.2–7.4), and the recovered BAL fluid (BALF) was immediately cooled to 4°C. For each mouse, the 4 BALF returns were centrifuged (500 *g* at 4°C), and the supernatant was removed for determination of total protein (an indicator of lung permeability; $n \geq 5$/group). Details of obtaining BALF differential cell counts and performing the Bradford protein assay have been published (27). Briefly, protein concentration was measured by the Bradford method (Bio-Rad, Hercules, CA, USA), according to the manufacturer's protocol. The cells were collected from the BALF by centrifugation and were resuspended in 0.5 ml of HBSS. The numbers of cells (per milliliter total BALF return) were counted with a hemocytometer as indicators of lung injury and inflammation. An aliquot (200 μl) of BALF cell suspension was cytocentrifuged (Shandon Southern Products, Pittsburgh, PA, USA) and stained with Wright-Giemsa stain (Diff-Quik; Baxter Scientific Products, McGaw Park, IL, USA) for differential cell analysis. Differential counts for epithelial cells, macrophages, and polymorphonuclear leukocytes (PMNs) were made by identifying 300 cells according to standard cytological techniques. Epithelial cells in particular were identified by the presence of cilia or as sheets of epithelium that are unique to neonatal BALF.

Lung histopathology

After euthanasia, the whole lung was fully inflated intratracheally *in situ* with zinc formalin (Fisher Scientific, Pittsburgh, PA, USA). The trachea was clamped and the lung removed and immersed in zinc formalin for 48 h. Fixed lungs were then placed in 70% ethanol until embedded, sectioned, and stained [hematoxylin and eosin (H&E)] for pathology assessment.

Heritability and correlation of phenotypes

Heritability estimates were calculated for each phenotype (28). The proportion of phenotype variation attributable to genetic background was determined by estimating the broad-sense heritability. Intrastrain correlations were estimated by the following formula:

$$r_1 = \frac{MS_B - MS_W}{MS_B + (n-1)MS_W}$$

where r_1 is the intrastrain correlation estimate, MS_B is the mean square of the between-strain comparison, MS_W is the mean square of the within-strain correlation, and n is the number of animals per strain.

Correlation of phenotypes was determined using Pearson's correlation coefficients (Gene Network, University of Tennessee, Knoxville, TN, USA; http://www.genenetwork.org).

GWA mapping

GWA mapping was performed on quantitative phenotype data by using 3 different algorithms: SNPster, a haplotype-based approach (Genomics Institute, Novartis Research Foundation, San Diego, CA, USA); efficient mixed-model association (EMMA), using individual single-nucleotide poly-

morphism (SNP) associations (University of California, Los Angeles, CA, USA); and FastMap (Carolina Environmental Bioinformatics Center, University of North Carolina, Chapel Hill, NC, USA). The algorithms underlying these approaches are described elsewhere (29–32). SNPster was initially used to determine the association of phenotype (mean BAL cell count or protein level for each strain) with haplotype structure throughout the mouse genome, because its algorithm is very conservative and usually generates lower $-\log_{10} P$ values relative to other haplotype association methods for identical associations because it includes family-wise error rates in the determination of $-\log_{10} P$ values for haplotype/phenotype associations. We then used the FastMap algorithm to determine whether we could replicate the findings of SNPster, because FastMap uses a similar haplotype structure approach. Furthermore, it performs permutation tests to calculate levels of genome-wide statistical significance for each 3-SNP window and associated analysis of variance (ANOVA) F statistic. EMMA was also used, because it is based on single SNP associations, rather than the 3-SNP haplotype, for lung response phenotypes of each mouse for each strain. It also corrects for genetic relatedness and population structure. We reasoned that if we identified the same QTLs with more than one of the algorithms, we would have greater confidence in our findings than if we used either of them alone. Only those QTLs identified with SNPster and one or both of the other approaches were included for further consideration. This procedure may have led to the exclusion of important associations, but it provided a strong rationale for moving forward on gene candidates. We used the conservative Bonferroni correction in **Table 3** to indicate whether the identified QTLs are significant or suggestive. $-\mathrm{Log}_{10} P$ values were considered significant if they exceeded 6.60 (genome-wide significance at $P<0.05$) and suggestive if they exceeded 6.06 (genome-wide suggestive at $P<0.20$). All of the strains have been genotyped to a level of ~630,000 SNPs. However, only a subset of the SNPs (between 200,000 and 230,000) were informative for haplotype association mapping with the strains of mice that were used in our analyses (*i.e.*, each haplotype had to be present in ≥10% of strains). Bonferroni corrections were calculated based on the 230,000 comparisons. Genes found within the QTLs were prioritized on the basis of whether nonsynonymous coding SNPs or promoter SNPs associate with differential responsiveness to hyperoxia exposure and biological plausibility.

We obtained the *Chrm2* haplotype from the Mouse Phenome Database (Jackson Laboratory; http://phenome.jax.org), and noninformative SNPs were removed (*i.e.*, no heterozygosity between strains or the minor allele was found in <10% of the strains). The strains were then arranged based on SNP similarity across the entire gene. The 3 haplotypes that were identified had ≥3 members (strains). Haplotypes with <3 members were not considered for statistical consideration, because a sample size of ≤2 is not appropriate. There are three 5′ and twenty-six 3′ untranslated region (UTR) SNPs in *Chrm2*, but none of them are associated with differential responses to hyperoxia among inbred strains, as we found with the nonsynonymous coding SNP, and they were not informative.

Statistics

Two-way ANOVA was used to evaluate the effects of exposure (air or hyperoxia) and strain (genotype) on disease phenotypes. Student-Newman-Keuls tests were used for *a posteriori* comparisons of the means. One-way ANOVA was used to compare the haplotype means, and Student's t test was used to compare the allelic group means in candidate genes. Statistical significance was accepted at $P < 0.05$.

RESULTS

Variation in hyperoxia-induced lung inflammation across strains of neonatal mice

Strain-specific responses were found in the hyperoxia-induced BALF phenotypes compared with the air-exposed controls (**Table 1**). For example, significant differences in mean BALF protein or PMNs were not found between the air- and hyperoxia-exposed 129S1/SvImJ mice (**Fig. 1*A*, *B*** and Table 1). In contrast, relative to their respective air-exposed controls, hyperoxia induced significantly greater increases in mean BALF protein and PMNs in the C3H/HeJ and PWD/PhJ neonatal mice than in the 129S1/SvImJ mice (Fig. 1*A*, *B* and Table 1).

Across all strains, significant interstrain variation was found for hyperoxia-induced differences in the mean number of BALF total cells relative to the air-exposed controls. Significantly more total cells were found after hyperoxia in a subset of strains (*e.g.*, 129S1/SvImJ, C57BL/10J, and NZW/LacJ) than in the air-exposed controls, whereas the other strains had reduced or unchanged BALF total cells (*e.g.*, I/LnJ, MOLF/EiJ, and CAST/EiJ; Table 1). The heritability of this phenotype was 47.6%.

Similar to BALF total cells, mean counts of hyperoxia-induced BALF macrophages, epithelial cells, and PMNs were significantly different across the strains of neonates (Table 1 and **Fig. 2**). Compared to counts in the respective air-exposed controls, the greatest increases in PMNs were found in the PWD/PhJ, P/J, and PWK/PhJ neonates, and the fewest PMNs were found in the BTBR T+tf/J, SWR/J, and RIIIS/J neonates (Fig. 2*A* and Table 1). The greatest mean counts of hyperoxia-induced BALF macrophages were found in the NZW/LacJ, BALB/cJ, and C57BL/10J neonates, and the lowest were found in the MOLF/EiJ, I/LnJ, and CAST/EiJ neonates (Fig. 2*B* and Table 1). Similarly, the greatest mean counts of hyperoxia-induced epithelial cells were found in the A/J, P/J, and C57BL/10J neonates, whereas the lowest were found in the MOLF/EiJ and I/LnJ neonates (Fig. 2*C* and Table 1). Heritability estimates of the BALF cell types were 39.8% (epithelial cells), 48.7% (PMNs), and 55.7% (macrophages).

Compared to levels in the respective air-exposed controls, hyperoxia caused significant increases in mean BAL protein concentration in all strains (Table 1). However, the amount of hyperoxia-induced increase in BAL protein varied significantly between strains, ranging from 64.3 ± 5.4 μg/ml in the BALB/cByJ to 249.1 ± 16.5 μg/ml in the C3H/HeJ (Fig. 2*D* and Table 1) strain. The intra- and interstrain variations in the BAL protein response to room air and hyperoxia exposure was greater than those in the other BAL phenotypes. Consequently, the heritability estimate for BAL protein was the lowest (33.6%) among all phenotypes.

TABLE 1. *Differential hyperoxic lung injury phenotypes in neonates from 36 strains of inbred mice*

		Protein (μg/ml)		Total cells		Neutrophils (%)		Macrophages		Epithelial cells	
Strain	Parameter	Air	O_2	Air	O_2	Air	O_2	Air	O_2	Air	O_2
129 × 1/SvJ	Mean	70.7	98.6*	33,333	35,833	0.08	2.48*	21,894	24,362	5,578	4,557*
	SEM	10.6	9.9	4,278	4,345	0.08	0.28	2,547	1,681	1,568	423
	n	6	9	6	9	4	7	4	7	4	7
129S1/SvImJ	Mean	71.8	109.3	36,806	53,194#	0.19	2.72*	27,608	40,730#	5,367	7,523#
	SEM	9.7	10.4	4,654	4,349	0.12	0.44	3,749	4,645	795	1,054
	n	9	18	9	18	7	13	7	13	7	13
A/J	Mean	46.4	95.6*	17,500	30,769	1.18	3.11*	13,978	34,097	2,395	11,001#
	SEM	2.7	12.3	1,887	5,134	0.64	0.77	1,446	3,409	446	2,467
	n	9	14	9	13	4	6	4	6	4	6
AKR/J	Mean	60.2	89.4*	20,673	24,688	5.44	5.38*	14,621	19,674	2,703	5,651*
	SEM	4.4	6.8	1,881	1,405	0.73	0.82	1,588	1,504	468	756
	n	13	16	13	16	3	7	3	7	3	7
BALB/cBy	Mean	35.2	64.3*	24,063	24,853	1.46	5.11*	21,766	2,4932	3,282	3,994*
	SEM	8.0	5.4	1,866	1,991	0.59	1.74	1,073	2,592	146	1,026
	n	4	17	4	17	5	6	5	6	5	6
BALB/cJ	Mean	28.4	80.6*	39,375	39,643	0.47	4.62*	33,061	43,929#	6,292	7,167
	SEM	1.7	6.3	3,576	1,864	0.08	0.67	4,076	4,913	843	774
	n	6	8	6	7	5	7	5	7	5	7
BTBR T+tf/J	Mean	76.2	111.1	31,750	28,456	0.00	0.41*	24,981	16,904*	7,019	7,334#
	SEM	8.3	9.0	5,327	3,350	0.00	0.16	6,753	4,676	1,184	1,447
	n	13	16	10	17	5	9	5	9	5	9
BUB/BnJ	Mean	54.6	98.0*	10,313	26,111	0.17	3.54*	7,398	19,767	2,893	3,769*
	SEM	8.4	6.4	1,288	2,119	0.09	0.67	1,053	2,531	485	667
	n	8	8	8	9	9	8	8	8	8	8
C3H/HeJ	Mean	43.1	249.1#	12,692	37,938	1.74	13.30#	11,185	23,870	2,257	5,802
	SEM	8.0	16.5	1,216	4,227	0.33	1.02	1,670	3,047	373	570
	n	13	25	13	20	9	18	9	18	9	18
C57BL/10J	Mean	46.2	79.6*	62,292	61,136#	1.56	8.24	53,483	42,492#	6,635	13,647#
	SEM	6.1	10.0	6,385	3,897	0.53	1.21	5,875	3,540	981	1,389
	n	6	11	6	11	6	11	6	11	6	11
C57BL/6J	Mean	48.3	135.9	23,875	43,355	1.10	8.60	19,138	31,573	4,464	7,381#
	SEM	7.4	14.1	843	4,626	0.40	1.12	679	4,449	772	913
	n	12	19	10	19	10	19	10	19	10	19
C57BR/cdJ	Mean	72.8	92.1*	15,583	16,250*	0.53	5.07*	11,551	10,305*	4,940	3,769*
	SEM	7.5	8.6	1,156	1,021	0.17	0.63	1,113	916	676	373
	n	13	22	15	22	10	15	10	15	10	15
C57L/J	Mean	46.3	183.9#	14,896	27,679	0.13	7.50	11,342	21,072	3,317	5,381*
	SEM	9.3	25.1	1,527	1,925	0.06	3.29	2,044	2,581	521	884
	n	12	14	12	14	7	8	7	8	7	8
C58/J	Mean	63.4	154.3	34,554	34,803	1.56	11.44	24,859	25,410	9,191	7,765#
	SEM	3.8	10.5	4,599	3,031	0.57	1.42	6,688	2,558	1,470	766
	n	14	19	14	19	8	14	8	14	8	14
CAST/EiJ	Mean	85.1	104.3*	11,000	11,458*	4.80	8.52	7,584	7,064*	2,680	3,154*
	SEM	17.1	26.4	1,000	1,528	1.78	3.05	1,068	1,049	286	736
	n	7	6	5	6	4	5	4	5	4	5
CBA/J	Mean	36.3	102.1*	23,000	26,375	0.09	9.88	17,851	23,320	2,663	4,373*
	SEM	4.6	13.2	2,682	2,792	0.09	1.98	2,374	2,540	199	837
	n	10	9	10	10	7	5	7	5	7	5
CE/J	Mean	82.0	157.5	17,404	24,438	0.34	5.76	6,424	14,326*	2,271	5,265*
	SEM	5.1	7.3	2,353	1,588	0.21	0.56	730	1,625	218	394
	n	12	19	13	20	5	11	5	11	5	11
DBA/2J	Mean	68.3	181.1#	18,750	25,703	1.00	5.42	14,412	18,159	3,920	4,531*
	SEM	10.6	22.9	1,518	2,848	0.38	0.95	1,800	2,400	451	497
	n	16	17	16	16	10	12	10	12	10	12
FVB/NJ	Mean	101.2	202.1#	15,000	37,981	2.38	8.71	13,037	29,737	3,225	7,271
	SEM	16.3	19.3	1,869	3,332	1.19	1.12	2,533	2,863	517	1,344
	n	11	13	11	13	7	11	7	11	7	11
I/LnJ	Mean	39.4	181.8#	8,125	7,505*	1.40	13.20#	5,481	3,970*	23,856	2,128
	SEM	3.7	19.9	360	319	0.21	2.16	454	218	193	557
	n	4	6	4	6	4	6	4	6	4	6

(continued on next page)

TABLE 1. *(continued)*

Strain	Parameter	Protein (μg/ml)		Total cells		Neutrophils (%)		Macrophages		Epithelial cells	
		Air	O_2	Air	O_2	Air	O_2	Air	O_2	Air	O_2
KK/HlJ	Mean	68.3	142.1	15,625	22,353	0.00	5.58*	10,725	12,729*	3,025	5,619*
	SEM	12.6	11.5	2,113	1,711	0	2.86	1,475	2,366	225	190
	n	8	17	8	17	3	4	3	4	3	4
MA/MyJ	Mean	108.3	184.7#	19,167	17,763*	2.27	5.43*	14,369	11,501*	4,698	4,356*
	SEM	11.8	22.6	1,758	1,561	1.22	1.21	1,562	1,176	527	548
	n	9	19	6	19	5	11	5	11	5	11
MOLF/EiJ	Mean	89.0	116.3	16,250	9,722*	0.58	5.00*	10,806	2,996*	5348	1,783*
	SEM	33	21	2,339	1,455	0.38	1.69	1,682	454	926	777
	n	4	9	4	9	4	3	4	3	4	3
MRL/MpJ	Mean	77.6	137.5	25,078	24,196	1.07	6.55	25,813	16,049*	7,131	5,967*
	SEM	8.4	9.0	1,994	1,270	0.30	1.01	6,899	1,791	1,464	712
	n	17	28	16	28	6	7	6	7	6	7
NOR/LtJ	Mean	68.4	161.9#	19,083	23,529	0.85	6.02*	19,861	15,041*	3,946	7,284
	SEM	5.7	9.0	1,995	1,658	0.30	1.31	2,279	1,637	387	1,050
	n	15	17	15	17	4	5	4	5	4	5
NZO/HlLtJ	Mean	67.1	157.5#	19,583	19,844*	2.23	8.90	15,703	13,301*	3,432	5,059*
	SEM	4.6	7.1	2,732	3,138	0.29	4.08	1,742	2,756	878	1,249
	n	3	7	3	8	3	4	3	4	3	4
NZW/LacJ	Mean	79.7	148.1	37,188	52,250#	0.25	7.28	32,965	46,611#	6,359	6,413
	SEM	7.0	8.7	3,673	6,957	0.17	2.94	4,250	7,970	1,301	762
	n	8	10	8	10	4	7	4	7	4	7
P/J	Mean	92.1	136.7	8,875	20,987	3.67	18.07#	8,824	12,417*	4,492	11,754#
	SEM	12.5	15.5	1,723	4,579	0.79	5.30	2,382	3,944	1,223	4123
	n	11	21	10	19	7	7	7	7	7	7
PL/J	Mean	86.3	173.9#	24,531	25,417	6.00	6.15	21,213	16,614*	5,568	2,849*
	SEM	14.7	28.8	2,302	1,916	5.02	1.29	318	2,710	1,331	622
	n	8	15	8	15	3	9	3	9	3	9
PWD/PhJ	Mean	58.6	166.1#	12,375	24,375	5.48	17.85#	8,555	13,834*	3,379	5,638*
	SEM	13.4	24.7	1,782	2,767	2.75	2.80	1,591	2,648	858	443
	n	10	14	10	12	4	10	4	10	4	10
PWK/PhJ	Mean	55.8	167.9#	10,446	17,188*	0.14	20.07#	6,595	9,996*	4,286	4,821*
	SEM	5.9	17.8	968	1,306	0.10	2.08	1,066	1,352	337	589
	n	15	27	14	28	7	16	7	16	7	16
RIIIS/J	Mean	84.4	88.8*	22,031	20,909	0.96	1.71*	13,610	14,098*	4,862	5,391*
	SEM	7.2	9.5	1,844	1,328	0.19	0.40	664	2,078	1,374	206
	n	8	10	8	11	5	7	5	7	5	7
SJL/J	Mean	57.1	104.6*	13,000	18,125*	2.26	8.96	8,890	9,304*	3,780	6,832
	SEM	7.1	15.5	1,090	3,143	0.73	1.47	773	1,982	432	148
	n	5	7	5	8	5	7	5	7	5	7
SM/J	Mean	37.3	112.9	14,688	17,143*	1.57	7.13	10,167	11,627*	2,665	3,016*
	SEM	3.0	16.1	1,386	1,630	0.47	0.99	546	1,041	205	155
	n	4	10	4	7	3	6	3	6	3	6
SWR/J	Mean	47.0	80.7*	30,938	51,618#	0.50	1.64	27,227	38,336#	3,560	8,980#
	SEM	7.5	11.6	2,571	6,033	0.22	0.46	2,666	6,036	200	1,072
	n	7	17	4	17	4	13	4	13	4	13
WSB/EiJ	Mean	35.9	85.0*	16,250	22,292	0.77	4.89*	15,061	16,485*	3,631	4,674
	SEM	3.1	13.3	4,705	2,509	0.77	1.42	5,012	1,515	687	806
	n	4	8	4	6	3	7	3	6	3	6

For each strain, the phenotypic mean, SEM, and sample size (*n*) for the phenotypes are listed. Air, filtered room air exposure for 4 d; O_2, 3 d of hyperoxia exposure. *$P < 0.05$ *vs.* highest-responding strain; #$P < 0.05$ vs. lowest-responding strain.

Correlation of hyperoxic lung injury phenotypes

We then asked whether disease phenotypes correlate across strains, to provide a better understanding of disease pathogenesis and potential mechanisms of injury. Mean BALF total, macrophage, and epithelial cell counts, but not PMN counts or protein level, correlated significantly with one another after air exposure (Pearson's *R* correlation coefficients; Supplemental Fig. S1). After exposure to hyperoxia, a weak but statistically significant correlation was found between PMNs and protein; total, macrophage, and epithelial cell counts also correlated significantly with one another (Supplemental Fig. S1).

Histopathology of hyperoxic lung injury in neonatal mice

Lung maturation and injury were compared by histopathology in the hyperoxia-nonresponsive 129S1/SvImJ neonates and the hyperoxia-responsive C3H/HeJ and

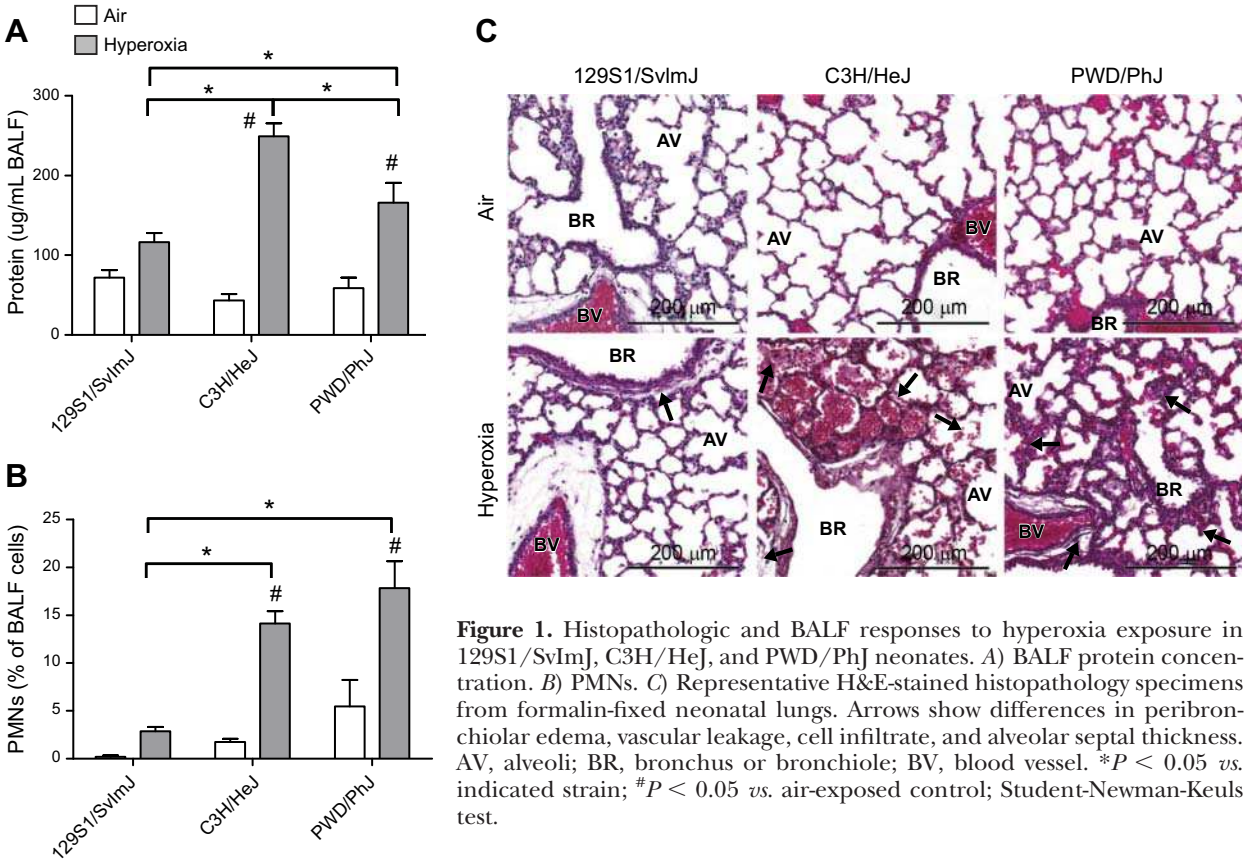

Figure 1. Histopathologic and BALF responses to hyperoxia exposure in 129S1/SvImJ, C3H/HeJ, and PWD/PhJ neonates. *A*) BALF protein concentration. *B*) PMNs. *C*) Representative H&E-stained histopathology specimens from formalin-fixed neonatal lungs. Arrows show differences in peribronchiolar edema, vascular leakage, cell infiltrate, and alveolar septal thickness. AV, alveoli; BR, bronchus or bronchiole; BV, blood vessel. $^{*}P < 0.05$ *vs.* indicated strain; $^{\#}P < 0.05$ *vs.* air-exposed control; Student-Newman-Keuls test.

PWD/PhJ neonates. Similar lung development (branched septae and multilobular alveoli) was found in each of the air-exposed strains by postnatal d 4 (Fig. 1*C*). However, strain-specific variation in lung injury was found after 72 h of hyperoxia. Minimal inflammatory cells and peribronchiolar edema were found in the hyperoxia-exposed 129S1/SvImJ neonates compared to those in the air-exposed controls. However, more severe injury, characterized by vascular leakage and inflammatory cell influx, was found in the C3H/HeJ lungs, whereas alveolar edema and thickened alveolar septae were found in the PWD/PhJ lungs.

Haplotype association mapping with disease phenotypes

To better understand the genetic basis of differential susceptibility to hyperoxia exposure in neonates, we used GWA mapping for each injury phenotype. Mapping of BALF macrophages by SNPster after hyperoxia exposure identified loci on chromosomes 4 and 7 with $-\log_{10} P > 5$ (**Table 2**). These same 2 loci were also identified by FastMap and EMMA and have been named hyperoxia susceptibility in neonatal lungs 1 (*Hsnl1*) and *Hsnl2*, respectively. Mapping of hyperoxia-induced increases in BALF PMNs with SNPster identified a peak on chromosome 6, with $-\log_{10} P$=4.60, and peaks on chromosomes 2 and 7, with $-\log_{10} P$=3.97 and 4.33, respectively (**Fig. 3** and Table 2). These 3 loci for the PMN phenotype were also identified by FastMap, with corresponding significant $-\log_{10} P$ = 7.48, 6.47, and 7.28, respectively (Table 2), and they have been named *Hsnl4*, *Hsnl3*, and *Hsnl5*. GWA analyses of other hyperoxia response phenotypes with SNPster did not identify peaks greater than $-\log_{10} P$ = 3.70 or were not confirmed with FastMap or EMMA.

We next queried the Mouse Phenome Database for informative SNPs in genes located within the QTLs, to determine whether any of them were associated with susceptibility to hyperoxia-induced lung injury. The minor allele SNPs must have been present in ≥10% of inbred strains to be considered for further analysis. Four cytochrome P450, family 2, subfamily j (*Cyp2j*) polypeptide genes, *Cyp2j11*, *Cyp2j6*, *Cyp2j9*, and *Cyp2j5*), were found in *Hsnl1*. Hyperoxia-induced changes in BALF macrophages were significant in strains homozygous for the minor allele SNPs, when compared to strains homozygous for the major allele (Table 3). In *Hsnl2*, nonsynonymous coding SNPs were found in *O*-6-methylguanine-DNA methyltransferase (*Mgmt*), and they significantly associated with differential susceptibility to hyperoxia among the 36 strains.

We used the same search strategy to query *Hsnl4* for hyperoxia susceptibility genes, and *Chrm2* was found directly beneath the peak of *Hsnl4* (Fig. 3*B*). The haplotype structure for synonymous and nonsynonymous coding SNPs was investigated, and 3 *Chrm2* haplotypes were identified (**Fig. 4*A***). Significantly greater hyperoxia-induced increases in BALF PMNs were found in the mice with *Chrm2* haplotype 1 than in those

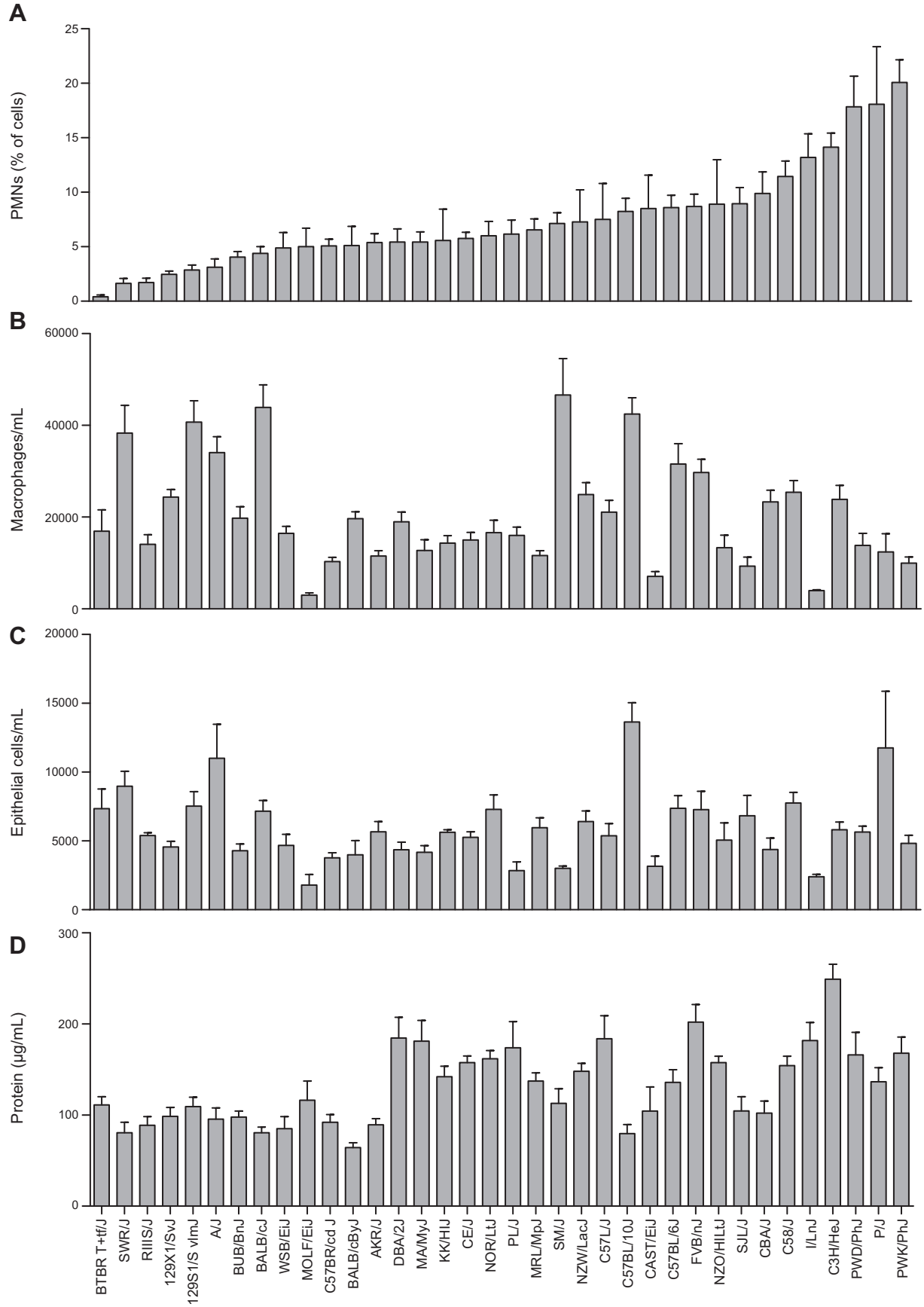

Figure 2. Strain distribution patterns of lung injury phenotypes from BALF after 72 h exposure to hyperoxia. *A*) PMNs as a percentage of BALF total cells. *B*) Macrophages per milliliter BALF. *C*) Epithelial cells per milliliter BALF. *D*) Protein concentration in BALF). Bars represent means ± SEM (n=5–28/strain).

TABLE 2. *QTLs and $-log_{10}$ P values for hyperoxia-induced inflammation identified by haplotype association mapping in 36 neonatal inbred mouse strains*

Phenotype and chromosome	QTL	QTL type	Location (Mb)	$-\text{Log}_{10}$ P	
				SNPster	FastMap
Macrophages					
4	*Hsnl1*	Significant	95.963320–97.095051	5.95	6.88
7	*Hsnl2*	Suggestive	143.452455–145.619658	5.38	6.30
Neutrophils					
2	*Hsnl3*	Suggestive	125.157670–129.353319	3.97	6.47
6	*Hsnl4*	Significant	35.750448–36.712935	4.60	7.48
7	*Hsnl5*	Significant	103.108764–109.235511	4.33	7.28

QTLs were given the name hyperoxia susceptibility in neonatal lungs (*Hsnl*). Genome-wide significant or suggestive association was determined by Bonferroni corrections for multiple testing (see Materials and Methods for details).

with haplotypes 2 or 3, and the PMN response to hyperoxia was significantly greater in the mice with *Chrm2* haplotype 2 than in those with haplotype 3 (Fig. 4*B*). Furthermore, the nonsynonymous C→T coding SNP (rs30378838; 36.474006 Mb) in exon 1 causes replacement of the proline residue at position 265 with leucine. Significantly reduced BALF PMN counts were found in the mice homozygous for T allele (9.6±0.9% PMNs/μl) compared to those in the strains homozygous for the C allele (4.2±0.6% PMNs/μl; Fig. 4*C* and Table 3).

We prioritized the subsequent investigation of these candidate genes on the basis of biological plausibility and strength of association of putative gene SNPs with responses to hyperoxia among the inbred strains (Table 3) and selected *Chrm2*. Moreover, the $Chrm2^{-/-}$ mouse had been developed (26) and was available for investigation in this model.

Targeted disruption of *Chrm2* reduces hyperoxia-induced lung injury

We further investigated *Chrm2* by comparing the pulmonary response to hyperoxia exposure in the $Chrm2^{+/+}$ and $Chrm2^{-/-}$ mice. We found statistically significant genotype, exposure, and interaction effects on BALF protein concentration (**Fig. 5*A***). Relative to respective air-exposed controls, mean BALF protein concentration was significantly increased in the $Chrm2^{+/+}$ neonates, but no increase was found in the $Chrm2^{-/-}$ neonatal lungs. Further, hyperoxia-induced BALF protein concentration was significantly greater in the $Chrm2^{+/+}$ mice than in the $Chrm2^{-/-}$ mice. Moreover, increased alveolar edema, thickening of the bronchial epithelium, and alveolar septae proliferation were found in the $Chrm2^{+/+}$ compared with the $Chrm2^{-/-}$ neonates after hyperoxia (Fig. 5*B*). Hyperoxic effects were found for other phenotypes (*e.g.*, BALF PMNs), but no genotype effects were detected.

DISCUSSION

Despite decades of research on the role of oxidant injury in neonatal lung disease, differential susceptibility remains poorly understood. This is the first study to evaluate hyperoxia-induced lung injury phenotypes in neonates across a genetically diverse panel of inbred strains of mice. Notably, strain distribution patterns of injury phenotypes in neonates did not replicate those in adult inbred mice exposed to hyperoxia. For example, neonatal C3H/HeJ mice were characterized as hyperoxia-responsive for inflammatory reactions in the present study, but C3H/HeJ mice were resistant to hyperoxic lung injury in a previous study of 6 strains of adult male mice (33). Similarly, hyperoxia-induced hyperpermeability was significantly increased in adult male BALB/cJ and C57BL/10J mice (33), whereas increases in BALF protein were minimal in neonates. Increased survival times were also found in adult female C3H/HeJ mice compared with other strains, such as 129S1/SvImJ, which we found to be resistant as neonates (34). Vancza *et al.* (35) also found age-dependent effects after ozone (O_3) exposure: C3H/HeJ neonates were very susceptible to O_3 as neonates but resistant as adults. These observations suggest that susceptibility mechanisms differ between adults and neonates.

The neonatal mouse lung at full term is undergoing saccular lung development that is comparable to that of the preterm human lung and very different from that of a mature adult lung. This study was designed to identify genetic factors that may have a role in neonatal lung injury, and we have demonstrated that it is important to consider the interaction between hyperoxia exposure with lung growth and development in the neonates as an important cofactor for hyperoxic lung injury. We also found that few strains (*e.g.*, PWD/PhJ and C3H/HeJ) had severe lung injury, and most of the strains had moderate, yet different, responses to the measured phenotypes. This finding is similar to clinical observations, as few preterm infants develop chronic lung disease or BPD after treatment with oxygen and respiratory support.

We further demonstrated that the strain distribution pattern for each of the quantitative phenotypes was continuous, which suggests that multiple genes contribute to the injury phenotypes. The large and genetically diverse panel of inbred strains phenotyped in the present study enables leverage of a rich and expanding

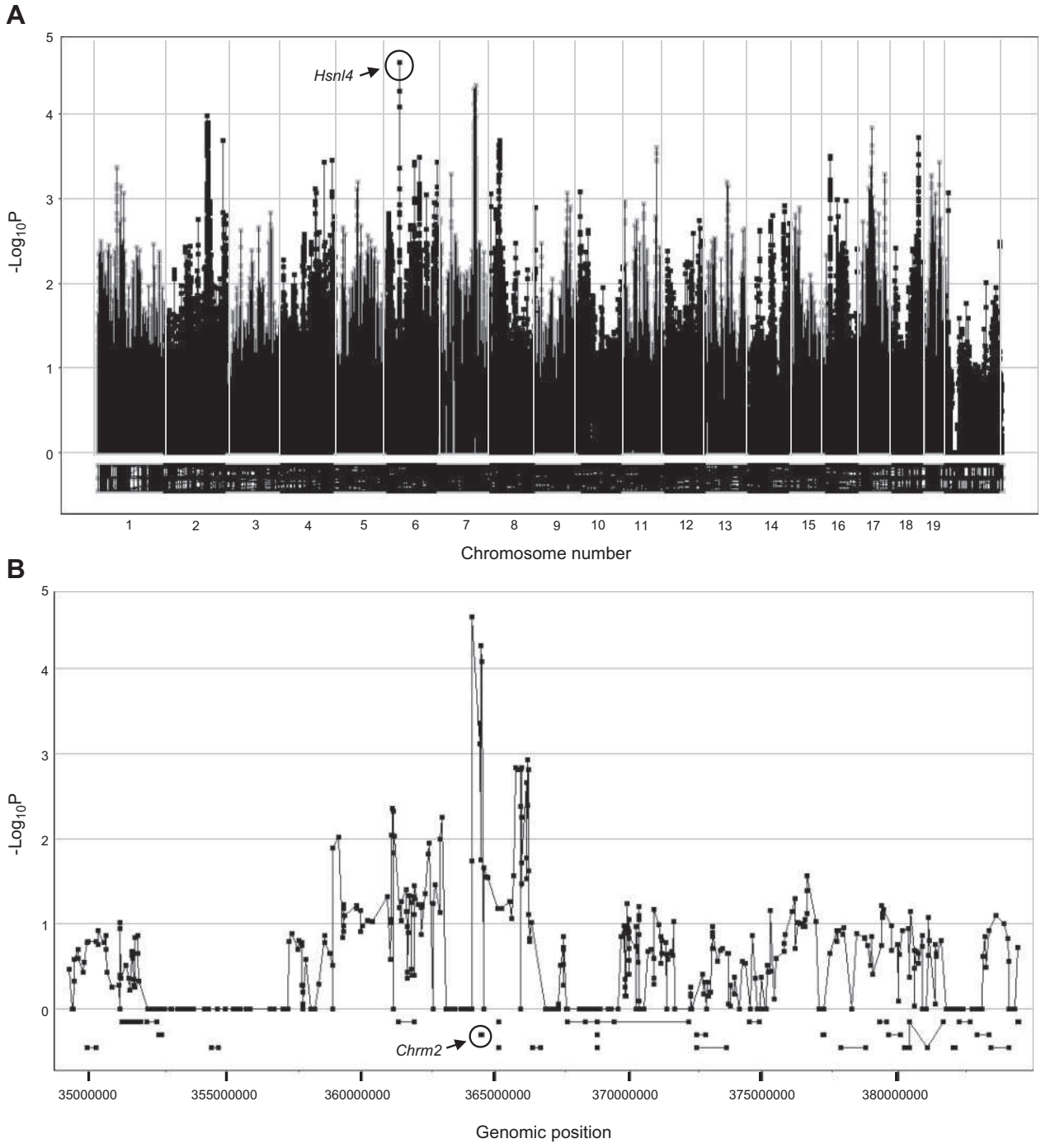

Figure 3. Genome-wide haplotype association map of BALF PMNs in 36 inbred strains of neonatal mice exposed to hyperoxia. *A*) Manhattan plot for hyperoxia-induced BALF PMNs (percentage of BALF total cells). Cumulative genomic position is on the *x* axis; $-\log_{10} P$ values are on the *y* axis. Circled rectangle (chromosome 6) identifies a locus with a $-\log_{10} P$ value of 4.60, indicative of association with hyperoxia-induced PMN infiltration. *B*) Enlarged view of the chromosome 6 locus identified by GWA of the PMN response to hyperoxia in inbred strains of mice and the underlying gene *Chrm2*.

SNP database for genetic analyses. Our analyses in an age-relevant animal model identified novel QTLs with several candidate susceptibility genes that associate with disease phenotypes. Candidate genes were limited to those having promoter or nonsynonymous coding SNPs as a means for prioritization; however, this does not imply that intronic SNPs are not important. Among the candidate susceptibility genes of interest are *Cyp2j6*, *Mgmt*, and *Chrm2* because of their biological plausibility in oxidative- and immune-mediated stress responses. *Cyp2j6* has been implicated as an anti-inflammatory mediator in acute allergic airway inflammation in ovalbumin-challenged mice and has a human orthologue, *CYP2J2* (36, 37). Furthermore, studies of human CYP2J2 *in vitro* have demonstrated that its activity associated with peroxisome proliferator-activated re-

A

		Haplotype 1			Haplotype 2																	Haplotype 3															
SNP ID	SNP annotation	MOLF/EiJ	PWD/PhJ	PWK/PhJ	C3H/HeJ	C57BL/10J	C57BL/6J	C57BR/cdJ	C57L/J	C58/J	CBA/CaJ	CE/J	I/LnJ	MA/MyJ	MRL/MpJ	NZO/HILtJ	NZW/LacJ	P/J	SJL/J	SM/J	WSB/EiJ	129S1/SvImJ	129X1/SvJ	A/J	AKR/J	BALB/cByJ	BALB/cJ	BTBRT + tf/J	BUB/BnJ	DBA/2J	FVB/NJ	KK/HIJ	NOR/LTJ	PL/J	RIIIS/J	SWR/J	CAST/EiJ
rs47611062	Cs L126	A	A	a	A	a	A	a	a	a	a	a	a	a	a	a	A	a	a	a	A	A	a	A	A	A	a	A	a	A	A	A	A	a	a	a	G
rs49264138	Cs V224	G	G	g	G	g	G	g	g	g	g	g	g	g	g	g	G	g	g	g	G	G	g	G	G	G	g	G	g	G	G	G	G	g	g	g	A
rs30267110	Cs P232	C	C	c	G	g	G	g	g	g	g	g	g	g	g	g	G	g	g	g	G	C	c	C	C	C	c	C	c	C	C	C	C	c	c	c	G
rs30378838	Cn P265L	C	C	c	C	c	C	c	c	c	c	c	c	c	c	c	C	c	c	c	C	T	t	T	T	T	t	T	t	T	T	T	T	t	t	t	C
rs30753439	Cs N283	T	T	t	C	c	C	c	c	c	c	c	c	c	c	c	C	c	c	c	C	T	t	T	T	T	t	T	t	T	T	T	T	t	t	t	C
rs30559117	Cs S289	C	C	c	T	t	T	t	t	t	t	t	t	t	t	t	T	t	t	t	T	C	c	C	C	C	c	C	c	C	C	C	C	c	c	c	C
rs30466951	Cs V346	T	T	t	G	g	G	g	g	g	g	g	g	g	g	g	G	g	g	g	G	T	t	T	T	T	t	T	t	T	T	T	T	t	t	t	G
rs47765394	Cs K375	G	G	g	G	g	G	g	g	g	g	g	g	g	g	g	G	g	g	g	G	G	g	G	G	G	g	G	g	G	G	G	G	g	g	g	A

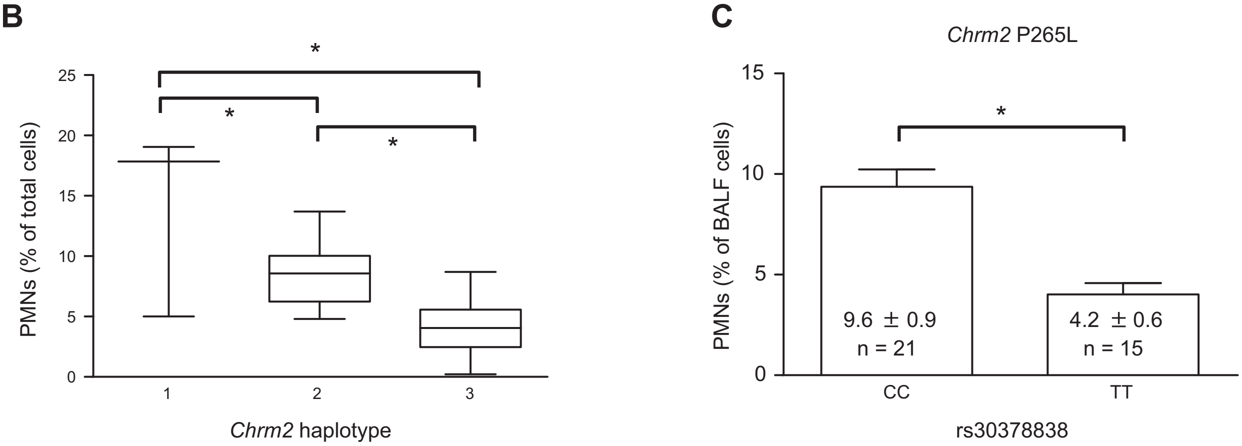

Figure 4. Haplotype structure of *Chrm2* and the association with susceptibility to hyperoxia-induced neutrophilia in BALF in inbred neonatal mice. *A*) Truncated haplotype structure of *Chrm2* with synonymous (Cs) and nonsynonymous (Cn) coding SNPs in strains of mice with similar haplotype. Uppercase symbols represent validated nucleotides. Lowercase symbols represent imputed nucleotides. *B*) Mean number of PMNs in strains of mice with the *Chrm2* haplotypes 1 (CCT; n=3 strains), 2 (GCC; n=17 strains), and 3 (CTT; n=14 strains). *$P < 0.05$, Student-Newman-Keuls test. *C*) Mean number of BALF PMNs for strains (n=21) homozygous for the rs30378838 C allele and strains (n=15) homozygous for the T allele. *$P < 0.05$; *t* test.

ceptor (PPAR)α and PPARγ activation and NF-κB and matrix metalloproteinase 9 inhibition (38–40).

Another candidate gene, *Mgmt*, encodes *O*-6-methylguanine-DNA methyltransferase, which is involved in DNA repair, and polymorphisms have been described in various cancers and contribute to epigenetic modifications (41). A specific role for *Mgmt* in development has not been elucidated, but it may have important implications, as epigenetic alterations play a critical part in developmental origins of lung disease (42). Joss-Moore *et al.* (42) demonstrated that mechanical ventilation with supplemental oxygen in neonates results in epigenetic changes that lead to altered expression of developmental genes, including elastin, vascular endothelial growth factor (VEGF), and PPARγ. Thus, further investigation of *Mgmt* polymorphisms may yield a novel epigenetic role for the gene in neonatal hyperoxic lung injury.

TABLE 3. *Candidate susceptibility genes in QTLs for hyperoxia-induced inflammation in neonatal mouse lungs*

		SNP					
QTL	Gene symbol	rs ID	Location (Mb)[a]	AA change	Major allele	Minor allele	*P*
Hsnl1	*Cyp2j11*	28105291	95.961592	I 476 V	T, 21.6 ± 1.8[a]	C, 7.7 ± 2.6[a]	0.0005
	Cyp2j6	28120055	96.202243	C 192 F	C, 21.6 ± 1.8[a]	A, 7.7 ± 2.6[a]	0.0005
	Cyp2j9	28119885	96.252622	I 90 V	T, 22.1 ± 1.8[a]	C, 7.6 ± 2.0[a]	0.0003
		28119867	96.257924	R 37 L	C, 21.8 ± 1.8[a]	A, 6.0 ± 1.6[a]	0.0003
	Cyp2j5	28119831	96.300844	P 394 T	C, 21.8 ± 1.8[a]	A, 6.1 ± 1.6[a]	0.0003
Hsnl2	*Mgmt*	33644808	144.143061	L 32 F	G, 22.1 ± 1.8[a]	T, 7.6 ± 2.0[a]	<0.0001
		33669425	144.277666	G 53 C	G, 24.8 ± 2.6[a]	T, 14.1 ± 1.5[a]	0.0030
Hsnl4	*Chrm2*	30378838	36.474006	P 265 L	C, 9.4 ± 0.9[b]	T, 4.0 ± 0.6[b]	<0.0001

Candidate susceptibility genes are indicated according to QTL. Locations are from build 37. All SNPs resulting in an amino acid (AA) change are listed for each gene. Phenotypic means ± SE for the respective QTL phenotype for strains having the major or minor allele are reported; *P* values indicate significant differences between allelic groups.[a]Macrophages $\times 10^3$. [b]Percentage PMNs.

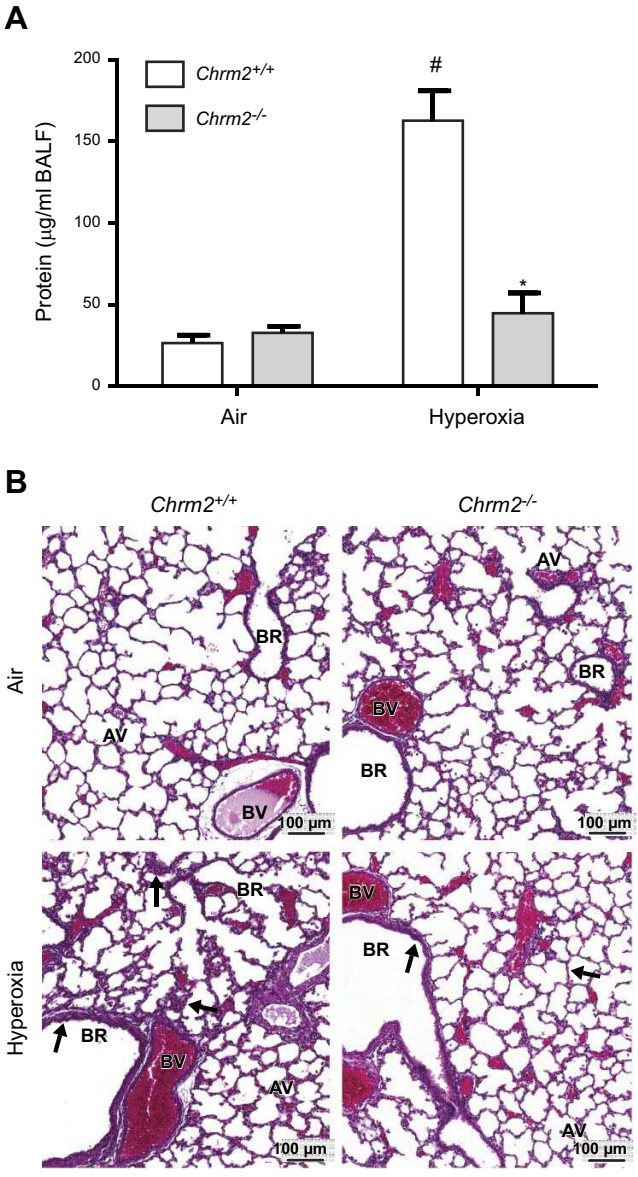

Figure 5. Differential pulmonary responses to hyperoxia exposure in *Chrm2*$^{+/+}$ and *Chrm2*$^{-/-}$ neonates. *A*) BALF protein concentrations. *B*) Representative H&E-stained histopathology images. Arrows indicate differences in alveolar edema and thickening of the bronchial epithelium and alveolar septae. AV, alveoli; BR, bronchus or bronchiole; BV, blood vessel. Bars represent means ± SEM (n=6–9/group). *$P < 0.05$ *vs.* *Chrm2*$^{+/+}$; #$P < 0.05$ *vs.* air; 2-way ANOVA.

Chrm2 encodes the M2 muscarinic acetylcholine receptor, a member of the muscarinic receptor family (M1–M5). All members of this receptor family belong to the superfamily of G-protein-coupled receptors. Muscarinic receptors modulate airway reactivity and have been studied in the pathogenesis of allergies and asthma (43). More recently, a new role of muscarinic receptors has been found in nonneuronal cholinergic signaling (44). Of particular interest are studies that reported the influence of muscarinic receptor activation on the release of proinflammatory cytokines in smooth muscle cells (45), bronchial epithelial cells (46), and alveolar macrophages (47). Specifically, human airway smooth muscle cells were found to secrete interleukin 8 when exposed *in vitro* to a muscarinic agonist and cigarette smoke extract (46). M2 muscarinic receptor expression differences have also been described in sputum samples from subjects with chronic obstructive pulmonary disease (45, 46). Although the effect of muscarinic receptor expression on pulmonary inflammatory cells is still unknown, neuroimmune crosstalk has recently been suggested as a regulatory mechanism of inflammation and infection (48, 49). For example, Rosas-Ballina *et al.* (48) found that acetylcholine acts on splenic macrophages to inhibit the production of proinflammatory tumor necrosis factor-α.

A potential role for *Chrm2* in differential susceptibility to hyperoxia-induced neonatal lung injury was supported by 2 lines of evidence. We initially found that both the haplotype structure of *Chrm2* and a nonsynonymous SNP (P265L) were associated with differential susceptibility to hyperoxia-induced inflammation and lung injury. The P265L substitution is found within the third intracellular loop of the receptor, a region known to be involved in receptor/G-protein coupling and regulation of receptor activity (50). Additional investigation is needed to validate the functional prediction. The second line of supportive evidence for *Chrm2* in hyperoxia susceptibility is that, relative to wild-type mice, targeted deletion of *Chrm2* significantly reduced hyperoxia-induced lung injury. Targeted deletion of *Chrm2* modulated hyperoxia-induced hyperpermeability rather than PMNs, the phenotype used to identify *Chrm2* by GWA mapping. We found only moderate hyperoxia-induced neutrophilia in wild-type and *Chrm2*$^{-/-}$ mice, and the difference between the strains was not significant. The lack of a genotype effect on the neutrophilia induced by hyperoxia may be attributable to the genetic background of the mice. Although hyperoxia-induced inflammation correlated with increased BALF protein concentrations in some strains, the 2 phenotypes did not correlate in others. Overall, among all strains, we have shown that these phenotypes have only a weak correlation (Fig. 2 and Supplemental Fig. S1). The role of strain background on the effects of gene mutation has been described in many other models (51–56). Investigators have found that the specific phenotypes attributed to a gene alteration in 1 strain of mouse were reduced or that additional subphenotypes were found in another strain of mouse due to different strain-specific gene penetrance. It is also possible that inflammation is sufficient for BAL protein changes in some strains, but not in others. Additional studies with *Chrm2* back-crossed to different inbred backgrounds are needed to address this question. Nevertheless, together these studies support the hypothesis that *Chrm2* has a role in the neonatal lung injury and inflammation phenotypes induced by hyperoxia. More studies are necessary to identify additional phenotypic effects of *Chrm2* deletion and the mechanisms through which *Chrm2* modulates hyperoxia response.

In summary, we have developed a genetic model of hyperoxia-induced lung injury in neonatal mice, with phenotypes that resemble some of those found in BPD. Furthermore, using GWA, we identified QTLs for inflammation phenotypes, which demonstrated that genetic background is an important determinant of susceptibility to hyperoxia-induced injury of the neonatal mouse lung and is likely to be age-dependent. Candidate susceptibility genes, including *Chrm2*, were identified in the QTLs. Results of studies with neonatal mice deficient in *Chrm2* were consistent with the hypothesis that *Chrm2* contributes to the pathogenesis of hyperoxic lung injury. Further investigation is needed to elucidate the role of other candidate susceptibility genes and to better understand the exact mechanism by which *Chrm2* modulates hyperoxia response and its relevance in human cohorts. Results of these studies have important implications for identifying the population at risk of neonatal lung injury and may provide therapeutic targets through which injury can be prevented. FJ

The authors thank L. M. DeGraff [National Institute of Environmental Health Sciences (NIEHS)], L. Perrow (NIEHS), and H. Price (Alion Science and Technology, McLean, VA, USA) for assistance with animal breeding and exposures; the NIEHS Histology Core for tissue processing and staining; and Drs. D. Cook and M. Fessler for critical review of the manuscript. This work was supported by a Director's Challenge Program and the Intramural Research Program, NIEHS, National Institutes of Health, U.S. Department of Health and Human Services. Author contributions: J.L.N., W.G., H.-Y.C., and S.R.K. conceived and designed the experiments; J.L.N., W.G., and K.C.V. performed the experiments; J.L.N., O.S., J.W., T.W., and K.C.V. analyzed the data; J.L.N. and S.R.K. wrote the paper; J.W. contributed animals.

REFERENCES

1. Northway, W. H., Jr., Rosan, R. C., and Porter, D. Y. (1967) Pulmonary disease following respirator therapy of hyaline-membrane disease: bronchopulmonary dysplasia. *N. Engl. J. Med.* **276,** 357–368
2. Jobe, A. H., and Bancalari, E. (2001) Bronchopulmonary dysplasia. *Am. J. Respir. Crit. Care Med.* **163,** 1723–1729
3. Bhandari, A., and Bhandari, V. (2009) Pitfalls, problems, and progress in bronchopulmonary dysplasia. *Pediatrics* **123,** 1562–1573
4. Jobe, A. H. (2011) The new bronchopulmonary dysplasia. *Curr. Opin. Pediatr.* **23,** 167–172
5. Parton, L. A., Strassberg, S. S., Qian, D., Galvin-Parton, P. A., and Cristea, I. A. (2006) The genetic basis for bronchopulmonary dysplasia. *Front. Biosci.* **11,** 1854–1860
6. Hallman, M., and Haataja, R. (2003) Genetic influences and neonatal lung disease. *Semin. Neonatol.* **8,** 19–27
7. Bose, C. L., Dammann, C. E., and Laughon, M. M. (2008) Bronchopulmonary dysplasia and inflammatory biomarkers in the premature neonate. *Arch. Dis. Child. Fetal Neonatal Ed.* **93,** F455–F461
8. Baraldi, E., Carraro, S., and Filippone, M. (2009) Bronchopulmonary dysplasia: definitions and long-term respiratory outcome. *Early Hum. Dev.* **85,** S1–S3
9. Parker, R. A., Lindstrom, D. P., and Cotton, R. B. (1996) Evidence from twin study implies possible genetic susceptibility to bronchopulmonary dysplasia. *Semin. Perinatol.* **20,** 206–209
10. Bhandari, V., and Gruen, J. R. (2006) The genetics of bronchopulmonary dysplasia. *Semin. Perinatol.* **30,** 185–191
11. Lavoie, P. M., Pham, C., and Jang, K. L. (2008) Heritability of bronchopulmonary dysplasia, defined according to the consensus statement of the national institutes of health. *Pediatrics* **122,** 479–485
12. Thompson, A., and Bhandari, V. (2008) Pulmonary biomarkers of bronchopulmonary dysplasia. *Biomark. Insights* **3,** 361–373
13. Bokodi, G., Treszl, A., Kovacs, L., Tulassay, T., and Vasarhelyi, B. (2007) Dysplasia: a review. *Pediatr. Pulmonol.* **42,** 952–961
14. Newton-Cheh, C., and Hirschhorn, J. N. (2005) Genetic association studies of complex traits: design and analysis issues. *Mutat. Res.* **573,** 54–69
15. Ohashi, J., and Tokunaga, K. (2001) The power of genome-wide association studies of complex disease genes: statistical limitations of indirect approaches using SNP markers. *J. Hum. Genet.* **46,** 478–482
16. Coalson, J. J., Winter, V. T., Siler-Khodr, T., and Yoder, B. A. (1999) Neonatal chronic lung disease in extremely immature baboons. *Am. J. Respir. Crit. Care Med.* **160,** 1333–1346
17. Hillman, N. H., Polglase, G. R., Pillow, J. J., Saito, M., Kallapur, S. G., and Jobe, A. H. (2011) Inflammation and lung maturation from stretch injury in preterm fetal sheep. *Am. J. Physiol. Lung Cell. Mol. Physiol.* **300,** L232–L241
18. Deng, H., Mason, S. N., and Auten, R. L., Jr. (2000) Lung inflammation in hyperoxia can be prevented by antichemokine treatment in newborn rats. *Am. J. Respir. Crit. Care Med.* **162,** 2316–2323
19. Saugstad, O. D. (2003) Bronchopulmonary dysplasia-oxidative stress and antioxidants. *Semin. Neonatol.* **8,** 39–49
20. Collard, K. J., Godeck, S., Holley, J. E., and Quinn, M. W. (2004) Pulmonary antioxidant concentrations and oxidative damage in ventilated premature babies. *Arch. Dis. Child. Fetal Neonatal Ed.* **89,** F412–416
21. Londhe, V. A., Sundar, I. K., Lopez, B., Maisonet, T. M., Yu, Y., Aghai, Z. H., and Rahman, I. (2011) Hyperoxia impairs alveolar formation and induces senescence through decreased histone deacetylase activity and up-regulation of p21 in neonatal mouse lung. *Pediatr. Res.* **69,** 371–377
22. Warner, B. B., Stuart, L. A., Papes, R. A., and Wispe, J. R. (1998) Functional and pathological effects of prolonged hyperoxia in neonatal mice. *Am. J. Physiol.* **275,** L110–L117
23. Dauger, S., Ferkdadji, L., Saumon, G., Vardon, G., Peuchmaur, M., Gaultier, C., and Gallego, J. (2003) Neonatal exposure to 65% oxygen durably impairs lung architecture and breathing pattern in adult mice. *Chest* **123,** 530–538
24. Flint, J., and Eskin, E. (2012) Genome-wide association studies in mice. *Nat. Rev. Genet.* **13,** 807–817
25. Gomeza, J., Shannon, H., Kostenis, E., Felder, C., Zhang, L., Brodkin, J., Grinberg, A., Sheng, H., and Wess, J. (1999) Pronounced pharmacologic deficits in M2 muscarinic acetylcholine receptor knockout mice. *Proc. Natl. Acad. Sci. U.S.A.* **96,** 1692–1697
26. Struckmann, N., Schwering, S., Wiegand, S., Gschnell, A., Yamada, M., Kummer, W., Wess, J., and Haberberger, R. V. (2003) Role of muscarinic receptor subtypes in the constriction of peripheral airways: studies on receptor-deficient mice. *Mol. Pharmacol.* **64,** 1444–1451
27. Cho, H. Y., van Houten, B., Wang, X., Miller-Degraff, L., Fostel, J., Gladwell, W., Perrow, L., Panduri, V., Kobzik, L., Yamamoto, M., Bell, D. A., and Kleeberger, S. R. (2012) Targeted deletion of *Nrf2* impairs lung development and oxidant injury in neonatal mice. *Antioxid. Redox Signal.* **17,** 1066–1082
28. Lightfoot, J. T., Turner, M. J., Daves, M., Vordermark, A., and Kleeberger, S. R. (2004) Genetic influence on daily wheel running activity level. *Physiol. Genomics* **19,** 270–276
29. Pletcher, M. T., McClurg, P., Batalov, S., Su, A. I., Barnes, S. W., Lagler, E., Korstanje, R., Wang, X., Nusskern, D., Bogue, M. A., Mural, R. J., Paigen, B., and Wiltshire, T. (2004) Use of a dense single nucleotide polymorphism map for in silico mapping in the mouse. *PLoS Biol.* **2,** e393
30. McClurg, P., Pletcher, M. T., Wiltshire, T., and Su, A. I. (2006) Comparative analysis of haplotype association mapping algorithms. *BMC Bioinformatics* **7,** 61
31. Gatti, D. M., Shabalin, A. A., Lam, T. C., Wright, F. A., Rusyn, I., and Nobel, A. B. (2009) FastMap: fast eQTL mapping in homozygous populations. *Bioinformatics* **25,** 482–489
32. Kang, H. M., Zaitlen, N. A., Wade, C. M., Kirby, A., Heckerman, D., Daly, M. J., and Eskin, E. (2008) Efficient control of

population structure in model organism association mapping. *Genetics* **178,** 1709–1723
33. Hudak, B. B., Zhang, L. Y., and Kleeberger, S. R. (1993) Inter-strain variation in susceptibility to hyperoxic injury of murine airways. *Pharmacogenetics* **3,** 135–143
34. Prows, D. R., Hafertepen, A. P., Gibbons, W. J., Jr., Winterberg, A. V., and Nick, T. G. (2007) A genetic mouse model to investigate hyperoxic acute lung injury survival. *Physiol. Genomics* **30,** 262–270
35. Vancza, E. M., Galdanes, K., Gunnison, A., Hatch, G., and Gordon, T. (2009) Age, strain, and gender as factors for increased sensitivity of the mouse lung to inhaled ozone. *Toxicol. Sci.* **107,** 535–543
36. Stoilov, I., Krueger, W., Mankowski, D., Guernsey, L., Kaur, A., Glynn, J., and Thrall, R. S. (2006) The cytochromes P450 (CYP) response to allergic inflammation of the lung. *Arch. Biochem. Biophys.* **456,** 30–38
37. Ma, J., Bradbury, J. A., King, L., Maronpot, R., Davis, L. S., Breyer, M. D., and Zeldin, D. C. (2002) Molecular cloning and characterization of mouse CYP2J6, an unstable cytochrome P450 isoform. *Biochem. Pharmacol.* **64,** 1447–1460
38. Wray, J. A., Sugden, M. C., Zeldin, D. C., Greenwood, G. K., Samsuddin, S., Miller-Degraff, L., Bradbury, J. A., Holness, M. J., Warner, T. D., and Bishop-Bailey, D. (2009) The epoxygenases CYP2J2 activates the nuclear receptor PPARalpha in vitro and in vivo. *PLoS One* **4,** e7421
39. Moshal, K. S., Zeldin, D. C., Sithu, S. D., Sen, U., Tyagi, N., Kumar, M., Hughes, W. M., Jr., Metreveli, N., Rosenberger, D. S., Singh, M., Vacek, T. P., Rodriguez, W. E., Ayotunde, A., and Tyagi, S. C. (2008) Cytochrome P450 (CYP) 2J2 gene transfection attenuates MMP-9 via inhibition of NF-kappabeta in hyperhomocysteinemia. *J. Cell. Physiol.* **215,** 771–781
40. Cho, H. Y., Gladwell, W., Wang, X., Chorley, B., Bell, D., Reddy, S. P., and Kleeberger, S. R. (2010) Nrf2-regulated PPARγ expression is critical to protection against acute lung injury in mice. *Am. J. Respir. Crit. Care Med.* **182,** 170–182
41. Gu, F., Qureshi, A. A., Kraft, P., Guo, Q., Hunter, D. J., and Han, J. (2009) Polymorphisms in genes involved in DNA repair, cell growth, oxidative stress and inflammatory response, and melanoma risk. *Br. J. Dermatol.* **161,** 209–212
42. Joss-Moore, L. A., Albertine, K. H., and Lane, R. H. (2011) Epigenetics and the developmental origins of lung disease. *Mol. Genet. Metab.* **104,** 61–66
43. Verhein, K. C., Fryer, A. D., and Jacoby, D. B. (2009) Neural control of airway inflammation. *Curr. Allergy Asthma Rep.* **9,** 484–490
44. Gwilt, C. R., Donnelly, L. E., and Rogers, D. F. (2007) The non-neuronal cholinergic system in the airways: an unappreciated regulatory role in pulmonary inflammation? *Pharmacol. Ther.* **115,** 208–222
45. Oenema, T. A., Kolahian, S., Nanninga, J. E., Rieks, D., Hiemstra, P. S., Zuyderduyn, S., Halayko, A. J., Meurs, H., and Gosens, R. (2010) Pro-inflammatory mechanisms of muscarinic receptor stimulation in airway smooth muscle. *Respir. Res.* **11,** 130
46. Profita, M., Bonanno, A., Montalbano, A. M., Ferraro, M., Siena, L., Bruno, A., Girbino, S., Albano, G. D., Casarosa, P., Pieper, M. P., and Gjomarkaj, M. (2011) Cigarette smoke extract activates human bronchial epithelial cells affecting non-neuronal cholinergic system signalling in vitro. *Life Sci.* **89,** 36–43
47. Sato, E., Koyama, S., Okubo, Y., Kubo, K., and Sekiguchi, M. (1998) Acetylcholine stimulates alveolar macrophages to release inflammatory cell chemotactic activity. *Am. J. Physiol.* **274,** L970–L979
48. Rosas-Ballina, M., Olofsson, P. S., Ochani, M., Valdes-Ferrer, S. I., Levine, Y. A., Reardon, C., Tusche, M. W., Pavlov, V. A., Andersson, U., Chavan, S., Mak, T. W., and Tracey, K. J. (2011) Acetylcholine-synthesizing T cells relay neural signals in a vagus nerve circuit. *Science* **334,** 98–101
49. Trakhtenberg, E. F., and Goldberg, J. L. (2011) Immunology: neuroimmune communication. *Science* **334,** 47–48
50. Wess, J. (1996) Molecular biology of muscarinic acetylcholine receptors. *Crit. Rev. Neurobiol.* **10,** 69–99
51. Baleato, R. M., Guthrie, P. L., Gubler, M. C., Ashman, L. K., and Roselli, S. (2008) Deletion of CD151 results in a strain-dependent glomerular disease due to severe alterations of the glomerular basement membrane. *Am. J. Pathol.* **173,** 927–937
52. Leontyev, D., Katsman, Y., and Branch, D. R. (2012) Mouse background and IVIG dosage are critical in establishing the role of inhibitory Fcgamma receptor for the amelioration of experimental ITP. *Blood* **119,** 5261–5264
53. Tiozzo, C., Danopoulos, S., Lavarreda-Pearce, M., Baptista, S., Varimezova, R., Al Alam, D., Warburton, D., Rehan, V., De Langhe, S., Di Cristofano, A., Bellusci, S., and Minoo, P. (2012) Embryonic epithelial Pten deletion through Nkx2.1-cre leads to thyroid tumorigenesis in a strain-dependent manner. *Endocr. Relat. Cancer* **19,** 111–122
54. Van den Buuse, M., Martin, S., Holgate, J., Matthaei, K., and Hendry, I. (2007) Mice deficient in the alpha subunit of G(z) show changes in pre-pulse inhibition, anxiety and responses to 5-HT(1A) receptor stimulation, which are strongly dependent on the genetic background. *Psychopharmacology* **195,** 273–283
55. Wallace, J. M., Golcuk, K., Morris, M. D., and Kohn, D. H. (2009) Inbred strain-specific response to biglycan deficiency in the cortical bone of C57BL6/129 and C3H/He mice. *J. Bone Miner. Res.* **24,** 1002–1012
56. Xu, J., Gontier, G., Chaker, Z., Lacube, P., Dupont, J., and Holzenberger, M. (2014) Longevity effect of IGF-1R mutation depends on genetic background-specific receptor activation. *Aging Cell* **13,** 19–28

Received for publication December 18, 2013.
Accepted for publication February 18, 2014.